Journal of Applied Mechanics and Technical Physics, Vol. 39, No. 6, 1998

ANALYSIS OF NONLINEAR SOLUTIONS WITH MANY SINGULAR POINTS IN PROBLEMS OF SPATIAL DEFORMATION OF RODS

V. V. Kuznetsov and S. V. Levyakov

UDC 539.3

We consider an algorithm for obtaining numerical solutions of the geometrically nonlinear problems of spatial deformation of elastic rods in the presence of many singular points. The questions of the construction of bifurcation solutions and the stability of the found states of equilibrium are discussed. The results of a study of the nonlinear deformation and stability of a ring in the spatial formulation, which are supported by experimental data, are given.

1. The theory of kinematic groups [1] is aimed at constructing and studying the discrete analogs of the nonlinear models of deformable bodies, without restricting their displacements and rotations.

From the viewpoint of a study of the geometrically nonlinear behavior of elastic bodies, thin rods are of great interest, because in them more significant changes than in shells and plates easily occur in the initial configuration upon elastic deformation for a wide class of support conditions. The majority of investigations dealing with flexible rods consider a particular case of deformation, namely, plane curving [2–7]. Numerical algorithms for solving the problems of the nonlinear statics of rods in the spatial formulation were proposed in [8–10]. However, spatial curving investigations were restricted to the initial deformation site and one bifurcation solution corresponding to the first bifurcation point. The possibility of the existence of solutions with many singular points in the region of arbitrary displacements of rods was not yet studied.

In the present paper, the algorithm for studying the nonlinear deformation and stability of spatial rods is considered using the finite-element model [1] corresponding to the nonlinear Kirchhoff theory. In the rod calculation, the values of the coordinates and direction cosines of two attached vectors lying in the plane of the transverse cross section should be specified as the initial data for each node of the calculation scheme.

The nonlinear problem of the spatial elasticity of a circular ring loaded by four forces in its plane is solved. This problem for a thin cylindrical shell was investigated by Kuznetsov and Soinikov [11]. Here we show that as the shell is shortened and may be regarded as a thin ring, the diversity of the equilibrium configurations considerably increases, which is due to the appearance of new bifurcation points. The calculation results are compared with experimental data.

2. The problem of determination of the strain state of a rod is solved by the discrete-continuation method, which is a step-by-step process involving the iterative improvement of the solution at each step.

The state of the discrete model of a rod is characterized by N generalized coordinates and the external-load parameter, which is considered to be a desired parameter. The consideration of the equilibrium conditions leads to the set of equations of the Newton–Raphson method

$$\mathbf{H}^{k-1}\delta\mathbf{q}^k + \mathbf{w}^{k-1}\delta q_{N+1}^k + \mathbf{g}^{k-1} = 0, \tag{2.1}$$

where $\mathbf{g}$ and $\mathbf{H}$ are the gradient and Hessian matrix of the ensemble of finite elements, the components of the vector $\mathbf{w}$ are determined by the formula $w_i = \partial^2 W/\partial q_i \partial q_{N+1}$ $(i = 1, \ldots, N)$, the vector $\delta\mathbf{q}$ includes variations

Chaplygin Siberian Aviation Institute, Novosibirsk 630051. Translated from Prikladnaya Mekhanika i Tekhnicheskaya Fizika, Vol. 39, No. 6, pp. 148–153, November–December, 1998. Original article submitted March 31, 1997.

0021-8944/98/3906-0949 $20.00

of the coordinates of the nodes and the components of the nodal rotation vectors [1], δq_{N+1} is the increment of the load parameter, W is the potential of external forces, and the superscript k denotes the iteration number.

The solution of system (2.1) is sought in the form

$$\delta \mathbf{q}^k = \delta q_{N+1} \mathbf{x}^k + \mathbf{y}^k,$$

where $\mathbf{x}^k$ and $\mathbf{y}^k$ satisfy the systems

$$\mathbf{H}^{k-1}\mathbf{x}^k + \mathbf{w}^{k-1} = 0, \quad \mathbf{H}^{k-1}\mathbf{y}^k + \mathbf{g}^{k-1} = 0.$$

The increment of the load parameter is calculated by the formulas

$$\delta q^1_{N+1} = \pm \delta s / (1 + (\mathbf{x}^1)^t \mathbf{x}^1)^{1/2} \quad \text{for} \quad k = 1; \tag{2.2}$$

$$\delta q^k_{N+1} = -(\mathbf{x}^1)^t \mathbf{y}^k / (1 + (\mathbf{x}^1)^t \mathbf{x}^1) \quad \text{for} \quad k > 1, \tag{2.3}$$

where δs is the step of continuation. The sign in (2.2) determines the direction of motion along the curve of the states of equilibrium. Formulas for the determination of the deformed configuration of a discrete system from the found vector components $\delta \mathbf{q}^k$ are presented in [1].

In the motion along the curve of the state of equilibrium, the fixed-sign property of all angular minors of the matrix $\mathbf{H}^0$ is analyzed at each step. According to the Sylvester criterion, the state of equilibrium is stable if all the angular minors are defined positively and unstable otherwise. The zero value of one or more minors points to the existence of the critical point. The multiplicity of this point is determined by the number of simultaneously vanishing angular minors in $\mathbf{H}^0$. Since the process of solution is discrete, the change of the sign of the angular minors means the passage through the critical point. However, the sign alternation can indicate that one of the minors touches the zero. This situation is clarified by analyzing the behavior of the determinant of the matrix $\mathbf{H}^0$ at a fairly small step of continuation.

In the case of singular points, the matrix $\mathbf{H}^0$ is degenerate. The type of the singular point is determined depending on whether system (2) is compatible or not. If the system is incompatible, the general solution for $k = 1$ has the form

$$\delta \mathbf{q}^1 = \mu_i \mathbf{f}_i, \quad \delta q^1_{N+1} = 0 \quad (i = 1, \ldots, l < N), \tag{2.4}$$

where μ_i are arbitrary multipliers and $\mathbf{f}_i$ are the linearly independent nontrivial solutions of the homogeneous set $\mathbf{H}^0 \mathbf{f}_i = 0$ $(i = 1, \ldots, l)$. The vectors $\mathbf{f}_i$ determine the directions of continuation of the solution in the neighborhood of the singular point. The solution will be further refined using formula (2.3).

If system (2.1) is compatible for $\det \mathbf{H}^0 = 0$, the general solution is written in the form

$$\delta \mathbf{q}^1 = \delta q^1_{N+1} \mathbf{x}^1 + \mu_i \mathbf{f}_i \quad (i = 1, \ldots, l < N).$$

The solution can be continued in one of $(l+1)$ directions by means of (2.2) and (2.3) for $\mu_1 = \mu_2 = \ldots = \mu_l = 0$ or by (2.4) and (2.3) for $\delta q^1_{N+1} = 0$.

3. We consider the spectrum of nonlinear solutions in the problem of curving of a circular ring having a narrow rectangular cross section, which is compressed by four equidistant radial forces P. The following parameters of the problem are adopted: $L/h = 10$, $R/L = 10$, and $\nu = 0.3$, where L and h are the dimensions of the cross section, R is the radius of the ring, and ν is the Poisson ratio. The ring can be regarded as a very short cylindrical shell of length L. The design is partitioned into 40 finite rod elements of equal length. At each point of force application, two restrictions are introduced, one of which is imposed on the out-of-plane displacement of the ring, and the other on the displacement along the direction of the tangent to the axial line. Thus, the displacements only in the radial direction are allowed for the points of force application, and the rotation of the transverse cross sections remain free. We study a purely mathematical solution of the problem without eliminating the self-intersection of the ring.

Figure 1 shows the diagram of the states of equilibrium, where the displacement u of the point a, which is referred to the ring radius, is plotted as the abscissa, and the load parameter $\lambda = PR^2/EI$, where E is the Young modulus and $I = Lh^3/12$ is the smaller moment of inertia of the cross section, is plotted as the

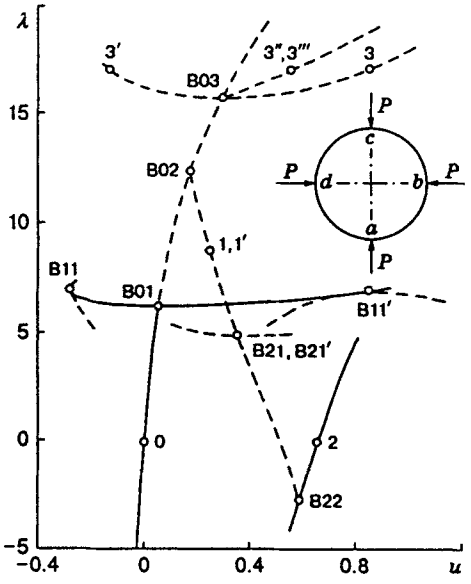

Fig. 1. Diagram of the states of equilibrium of the ring: solid and dashed curves refer to the steady and unstable stable of equilibrium, respectively.

ordinate. In essence, the projection of the deformation curves in the $(N+1)$-dimensional space onto the plane of the parameters λ and u is given.

The plane four-lobe configurations of the ring correspond to the basic deformation branch passing through the undeformed-state point 0. Three bifurcation points B01, B02, and B03 were found on the basic branch in the range of deflection variation ($0 < u < 1$). We consider each point and study the corresponding branches of the nonlinear solutions.

Point B01 was considered by Alfutov et al. [12] and Seide and Albano [13]. The critical value that we calculated, $\lambda_* = 6.155$, is close to $\lambda_* = 6.1104$ [13] found by an analytical method for an inelastic ring. At this point, the passage to the new steady states of equilibrium (the branch B11′–B01–B11) occurs. On this branch, the ring acquires the characteristic dumbbell-like shape keeping the double symmetry of deformation. Figure 2 shows the shape of the ring in the state corresponding to point B11 (it is rotated turned by 90° at B11′). For $\lambda_* = 6.902$ (the states corresponding to B11 and B11′), the repeated loss of stability caused by the lateral buckling of the elongated dumbbell-like configuration occurs. Its character is similar to the loss of stability of the Euler rod. This bifurcation point and the supercritical behavior of the ring were investigated by Kuznetsov and Soinikov in [3], where the critical load parameter was calculated with an error of 5.7%.

At point B02 ($\lambda_* = 12.318$), a transition to the spatial flexural–torsional equilibrium shapes is possible on the basic deformation branch. Figure 3 shows the ring shape calculated for $\lambda = 8.75$ (condition 1, Fig. 1). This shape of the supercritical deformation was found in [11] in analyzing the curving of a short cylindrical shell ($R/L = 1$) loaded by four radial forces. The calculations show that the branch of the solution describing the spatial deformation of the ring is a closed curve with four bifurcation points B02, B21, B21′, and B22; the last three were found for the first time. Figure 4 shows the diagram of the states of equilibrium in the plane of the parameters λ and w, where w is the displacement from the plane of the initial curvature of the ring, referred to the radius R, for a node equidistant from the points of force application a and b. In the motion along this branch of the states of equilibrium, $\det \mathbf{H}^0$ changes sign at bifurcation points B21 and B21′ and touches the zero at points B02 and B22. At points B21 and B21′ the transition occurs to the new spatial equilibrium shapes, which are not considered here. One more branch of steady plane equilibrium configurations passes through point B22. For example, in the state corresponding to point B22 ($\lambda_* = -2.810$) the ring takes the shape shown in Fig. 5. In the state corresponding to point 2 on this branch (see Fig. 1), which corresponds

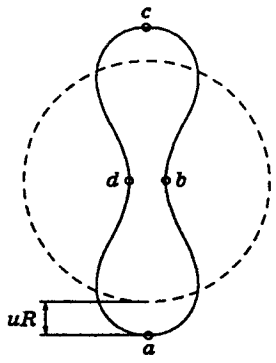

Fig. 2

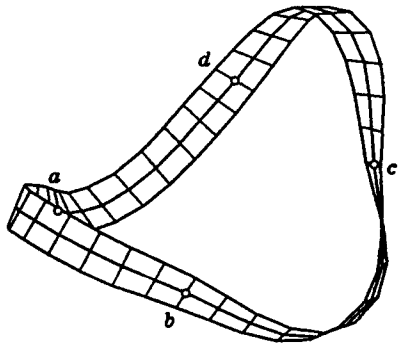

Fig. 3

Fig. 2. Dumbbell-like equilibrium configuration of the ring for $\lambda_* = 6.902$.

Fig. 3. Spatial flexural–torsional equilibrium configuration of the ring for $\lambda = 8.75$.

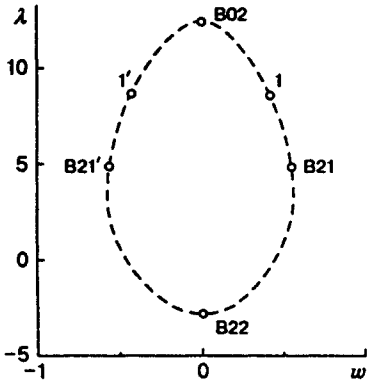

Fig. 4

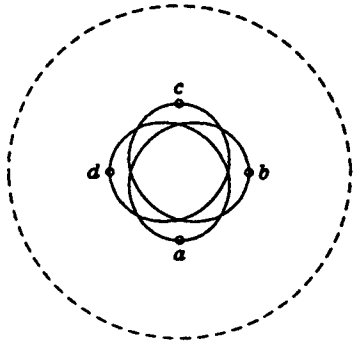

Fig. 5

Fig. 4. Diagram of the spatial states of equilibrium of the ring.

Fig. 5. Plane equilibrium configuration of the ring for $\lambda_* = -2.81$.

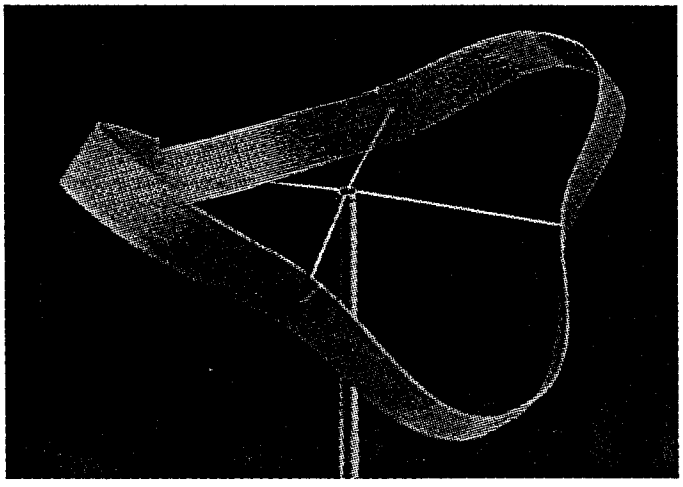

Fig. 6. Spatial configuration of the ring obtained in the experiment.

to the zero load, the ring takes the shape of a spiral inserted in a circle of radius $R/3$.

In contrast to the singular points considered, bifurcation point B03 ($\lambda_* = 16.670$) has multiplicity 2, i.e., two solutions bifurcate at this point (branches 3–B03–3′ and 3″–B03–3‴ in Fig. 1) to which correspond the plane equilibrium configurations.

The phenomenon of the loss of stability of the plane form of curving and the subsequent deformation of the ring can be reproduced in fragments in the experiment on a thin celluloid model loaded by four stretched radial filaments. Gradually increasing the tension of the filaments, one can observe a transition from plane four-lobe equilibrium configurations to spatial configurations of the ring. Figure 6 shows a deformation of the ring's state similar to that in Fig. 3. A subsequent loading causes a pop and, as a result, the ring tends to the state at point 2 (see Fig. 1) at which the tension of the filaments disappears. This configuration cannot be strictly reproduced in the experiment, because the dimensions of the transverse cross section of the model are finite.

The study of the problem in the spatial formulation by means of the developed algorithm has allowed us to reveal previously unknown singular points of the nonlinear solution, to study the deformation of the ring, and to determine the stability of the found states of equilibrium. The results do not cover all possible equilibrium configurations. These can be obtained by continuing the solution along the considered branches and, possibly, new singular points can be detected.

REFERENCES

1. V. V. Kuznetsov and S. V. Levyakov, "Kinematic groups and finite elements in solid-state mechanics," *Izv. Ross. Akad. Nauk, Mekh. Tverd. Tela*, No. 3, 67–82 (1994).
2. E. P. Popov, *Theory and Calculation of Flexible Elastic Rods* [in Russian], Nauka, Moscow (1986).
3. V. V. Kuznetsov and Yu. V. Soinikov, "Numerical solution of problems of nonlinear curving of plane rods," *Prikl. Mekh.*, **22**, No. 10, 91–98 (1986).
4. S. Srpcic and M. Saje, "Large deformations of thin curved plane beam of constant initial curvature," *Int. J. Mech. Sci.*, **28**, No. 5, 275–287 (1986).
5. R. E. Miller, "Numerical analysis of generalized plane elastica," *Int. J. Num. Meth. Eng.*, **15**, No. 3, 325–332 (1980).
6. Yu. M. Volchkov, G. V. Ivanov, and O. N. Ivanova, "Calculation of the plane equilibrium shapes of thin rods by the method of self-balanced residues," *Prikl Mekh. Tekh. Fiz.*, **35**, No. 2, 142–151 (1994).
7. É. I. Grigolyuk, "Nonlinear behavior of slanting rods, " *Dokl. Ross. Akad. Nauk*, **348**, No. 6, 759–763 (1996).

8. K. J. Bathe and S. Bolourchi, "Large displacement analysis of three-dimensional beam structures," *Int. J. Num. Meth. Eng.*, **14**, No. 7, 961–986 (1979).
9. K. S. Surana and R. M. Sorem, "Geometrically non-linear formulation for three-dimensional curved beam elements with large rotations," *Int. J. Num. Meth. Eng.*, **28**, No. 1, 43–73 (1989).
10. G. V. Ivanov and O. N. Ivanova, "Calculation of the spatial equilibrium configurations of thin elastic rods by the method of self-balanced residuals," *Prikl Mekh. Tekh. Fiz.*, **35**, No. 4, 130–136 (1994).
11. V. V. Kuznetsov and Yu. V. Soinikov, "Shell deformations in arbitrary displacements by the finite-element method," *Izv. Akad. Nauk SSSR, Mekh. Tverd. Tela*, No. 1, 131–138 (1987).
12. N. A. Alfutov, Yu. I. Klyuev, and V. V. Trofimov, "Stability of a circular ring under essentially nonaxisymmetrical loading," in: *Proc. of VIII All-Union Conf. on the Theory of Shells and Plates* (Rostov-on-Don) [in Russian] Nauka, Moscow (1971), pp. 209–213.
13. P. Seide and E. D. Albano, "Bifurcation of circular rings under normal concentrated loads," *Trans. ASME, Ser. E, J. Appl. Mech.*, **40**, No. 1, 233–238 (1973).